Chapter 8
Thermal Imaging and Infrared Sensing in Plant Ecophysiology

Hamlyn G. Jones

1 Introduction

1.1 Why Thermal Sensing?

Leaf temperature is important for plants both because of its effects on the rates of critical physiological processes and because of the damaging effects of temperature extremes. Notwithstanding these phenomena, remote estimation of leaf temperature also provides a powerful tool for the study of plant water relations and some other phenomena such as freezing. Most ecological and physiological applications of thermal remote sensing are based on the fact that the latent heat of vaporization required to evaporate from plant leaves is a major part of the leaf or canopy energy balance such that increasing evaporation or transpiration through the stomata leads to a cooling of the surface. The degree of cooling can therefore be used as an indicator of transpiration rate and stomatal opening, and hence as a measure of plant response to environmental stresses such as drought. A major practical problem in the application of this result in agriculture and in natural ecosystems is that, in addition to stomatal closure, many plant factors such as leaf orientation or reflectance and environmental factors such as radiation, wind speed and humidity also impact on leaf or canopy temperature over a rapid timescale. Practical application of this result for ecophysiological studies therefore requires approaches to allow for the various physiological and environmental determinants of canopy temperature (Jones 1999a, b, 2004), as will be discussed in detail below.

Thermal imaging also has applications in fields other than plant water relations. For example the high latent heat of fusion of water means that a large amount of heat

H. G. Jones (✉)
University of Dundee, Dundee, Scotland, UK

University of Western Australia, Crawley, WA, Australia
e-mail: h.g.jones@dundee.ac.uk

A. M. Sánchez-Moreiras, M. J. Reigosa (eds.), *Advances in Plant Ecophysiology Techniques*, https://doi.org/10.1007/978-3-319-93233-0_8

is released when plant tissue freezes and various workers have used thermal imaging to follow the (rapid) progress of freezing (Fuller and Wisniewski 1998; Hamed et al. 2000; Carter et al. 2001; Stier et al. 2003). Similarly, thermal dynamics can provide useful information at scales from the functioning of ecosystems (Bendoricchio and Jørgensen 1997; Aerts et al. 2004) through soil moisture content estimation (Verstraeten et al. 2006) to the aerodynamic properties of single leaves (Jones 2014).

The principles underlying the control of leaf temperature were formalised by the early 1960s (Raschke 1956, 1960) and, with the development of infrared thermometers, were first used for the study of plant water relations by Tanner and Fuchs (Tanner 1963; Fuchs and Tanner 1966). Extensive subsequent studies by Jackson, Idso and colleagues (1977, 1981; Idso 1982) promoted thermal sensing as a tool for irrigation scheduling.

The greatest uptake of thermal sensing, however, came with the widespread availability of thermal imaging and especially, from about the year 2000, uncooled microbolometer sensors that operate in the long-wave (c.9–14 μm) thermal infrared (Jones 2004). For thermal sensing in the field it is essential to use only imagers that operate in the long-wave thermal region rather than shorter wavelengths as the latter are much more subject to interference by reflected sunlight (Leigh et al. 2006). Imagery has many advantages over the use of point sensors, especially the possibility of multiple replication within an image, and the ability to ensure that the temperature is that of the material of interest (e.g. a leaf) without any contamination by background.

Thermal imagery can be used in several ways for ecophysiological purposes. The simplest is in a purely qualitative mode where visual comparison of temperatures of different canopies can be used to identify plants, or areas of vegetation, under particular stress (where those areas having particularly high temperatures indicate stomatal closure). The second mode is semi-quantitative, and is widely used in plant phenotyping and involves ranking plots or genotypes for temperature (and hence stomatal closure). The most powerful approach, however, involves quantitative application to estimation of stomatal conductance, evaporation rate or aerodynamic properties based on application of energy balance and measurement of the necessary meteorological variables.

1.2 Basic Energy Balance Calculations

Application of thermal sensing as an ecophysiological tool is largely based on an understanding of leaf or canopy energy balance. Useful summaries of the energy balance equations and their application to thermal imagery may be found in a number of texts (Monteith and Unsworth 2008; Jones and Vaughan 2010; Jones 2014) and reviews (Jones 2004; Maes and Steppe 2012).

For a plant leaf (or equivalently for a canopy) at any instant, the net energy fluxes into and out of the system must equal the rate of energy storage

$$\mathbf{R}_n - \mathbf{C} - \lambda\mathbf{E} = \mathbf{M} + \mathbf{S} \tag{8.1}$$

where $\mathbf{R}_n$, is the net heat gain from radiation, **C** is the net 'sensible' heat loss, $\boldsymbol{\lambda}\mathbf{E}$ is the net latent heat loss, **M** is the net heat stored in biochemical reactions (usually negligible) and **S** is the net physical storage. In the steady state net storage is zero, so the net radiation input is balanced by evaporative and sensible heat losses. All fluxes are expressed per unit leaf area as flux densities in W m^{-2}.

Leaf temperature affects all these fluxes, with sensible heat loss given by

$$\mathbf{C} = g_H \left(\rho c_p\right)\left(T_s - T_a\right) \tag{8.2}$$

where g_H is the leaf conductance to heat transfer, ρ is the density of air, c_p is the specific heat of air, T_s is the leaf temperature and T_a is the air temperature (Jones 2014).

Similarly one can write the evaporative heat loss as

$$\lambda\mathbf{E} = g_W \left(\rho c_p / \gamma\right)\left(D + \boldsymbol{s}\left(T_s - T_a\right)\right) \tag{8.3}$$

where g_W is the total conductance to water vapour, γ is the psychrometer constant, D is water vapour pressure difference between the inside of the leaf and the free air and $\boldsymbol{s}$ is the slope of the saturation vapour pressure-temperature curve.

Substituting these equations into the steady state energy balance and rearranging gives the leaf to air temperature difference as the following function of environmental and physiological variables:

$$T_s - T_a = \left(\gamma \mathbf{R}_n - g_W \rho c_p D\right) / \left(\rho c_p \left(g_H \gamma + g_W \boldsymbol{s}\right)\right) \tag{8.4}$$

It is convenient to eliminate the need for a direct measurement of the net radiation actually received by the leaf by using the concept of net isothermal radiation ($\mathbf{R}_{ni}$), defined as the net radiation that would be received if the leaf were at air temperature (Jones 2014), and rewriting Eq. (8.4) as

$$T_s - T_a = \left(\gamma \mathbf{R}_{ni} - g_W \rho c_p D\right) / \left(\rho c_p \left(g_{HR} \gamma + g_W \boldsymbol{s}\right)\right) \tag{8.5}$$

where g_{HR} is the parallel resistance to sensible heat and radiation.

2 Applications

2.1 Stress Indices and Normalisation of Leaf Temperature

A number of approaches have been used over the years to develop semi-quantitative approaches to normalisation of leaf or canopy temperature to account for variation in environmental conditions. One of the main drivers has been the wish to develop indicators of plant water-deficit stress as indicated by stomatal closure. The simplest

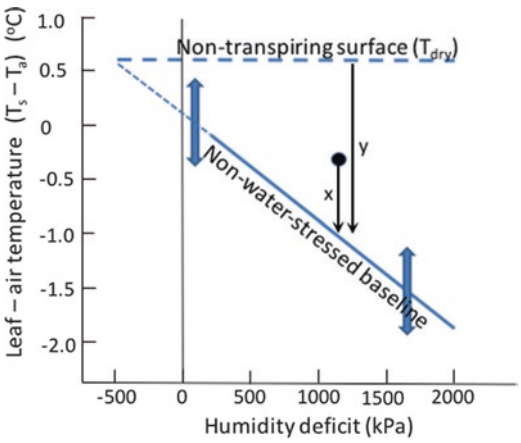

Fig. 8.1 Illustration of the calculation of CWSI. The non-water stressed baseline temperatures are obtained empirically for a given crop/site combination. The upper limit represents the temperature of a non-transpiring surface in the same environment. For any measured canopy temperature, CWSI is calculated as x/y. The two broad arrows indicate potential errors in temperature measurement and show that a given measurement error has a much greater relative impact on errors in CWSI in humid environments than in more arid situations

approach is to normalise data with reference to canopy air temperature, with early studies defining stress as the canopy-air temperature difference around mid-day (Jackson et al. 1977) or as the temperature difference between the canopy of interest and a comparable well-irrigated canopy (Gardner et al. 1981). More powerful was the introduction by Idso and colleagues (Jackson et al. 1981; Idso 1982) of a crop water stress index (CWSI; see Fig. 8.1) that takes account of variation in atmospheric humidity and makes use of the temperature of a notional non-transpiring canopy as well as the temperature of a well watered canopy transpiring at its potential rate (T_{nws}) using

$$\mathrm{CWSI} = \left(T_s - T_{nws}\right) / \left(T_{dry} - T_{nws}\right) \tag{8.6}$$

This approach has been very widely used since the 1980s for irrigation scheduling, but it suffers from a number of disadvantages that limit its application in ecological systems and in more humid or temperate climates. In particular it requires a standard empirical non-water stressed base line derived for a comparable crop in a similar environment, but does not take account of any potential variation in irradiance or wind speed, though extensions that overcome some of these limitations have been suggested (Keener and Kircher 1983). Another problem with this formulation is that it is very non-linearly related to evaporation rate or stomatal conductance, which are usually of most interest in plant water relations studies.

The use of actual physical references measured simultaneously by thermography is a particularly powerful approach to improvement of this approach that reduces

the effects of short-term environmental fluctuations. The use of reference surfaces to mimic dry or wet leaves (Brough et al. 1986; Qiu et al. 1996; Jones et al. 1997) allows one to eliminate the need for one or more of these environmental variables. Using such references having aerodynamic and radiative properties as similar as possible to real leaves, Jones (1999b) defined a stress index (SI_{CWSI}) analogous to Idso's CWSI, but using a wet surface as reference (with infinite surface conductance), rather than a well-watered vegetation surface. Importantly, this paper also proposed a 'conductance index' (SI_{gl}) that is proportional to stomatal conductance and can be expressed as

$$SI_{gl} = \left(T_{dry} - T_s\right) / \left(T_s - T_{wet}\right) \tag{8.7}$$

where T_{wet} is the temperature of a wet freely evaporating mimic leaf.

2.2 Use of Temperature Variance As a Stress Index

An alternative approach to the use of thermal data for the study of differences in stomatal conductance is based on the variability of temperature between different leaves in the canopy. This approach was proposed by Fuchs (1990) and is based on the idea that temperature variance increases as stomata close, because the importance of the radiative component of the energy balance increases as stomata close. This idea was further developed by Bryant and Moran (1999), who derived a histogram-derived crop water stress index (HCWSI) based on the skewness or kurtosis of the temperature frequency distribution. In principle the variance-based approaches will be most sensitive for sunlit leaves which maximise the temperature variation as compared with shaded leaves (Jones 2004). Unfortunately attempts to use these approaches have thus far had only variable success (Grant et al. 2007, 2016).

2.3 Stomatal Conductance and Evaporation

More quantitative data can be obtained by use of the full energy balance equation; for example Eq. (8.5) can be rearranged (Leinonen et al. 2006; Guilioni et al. 2008) to allow one to estimate the total conductance to water vapour according to

$$g_W = \gamma \left(\left(R_{ni} / \rho c_p \right) - g_{HR} \left(T_s - T_a \right) \right) / \left(s \left(T_s - T_a \right) + D \right) \tag{8.8}$$

Unfortunately, in addition to the requirement for an accurate estimate of leaf temperature use of this equation for estimation of conductance, requires information on air temperature, net radiation, humidity and boundary layer conductance

which are not all easy to estimate at the level of the leaf. Useful reductions in environmental data requirements can be obtained by using temperatures of the 'mimic' reference surfaces discussed above. For example, measurement of the temperature of a dry reference surface that mimics the radiative and aerodynamic properties of the transpiring leaves (T_{dry}) allows one to eliminate R_{ni} from Eq. (8.8), giving (Leinonen et al. 2006),

$$g_W = g_{HR}\gamma\left(T_{dry} - T_s\right)/\left(s\left(T_s - T_a\right) + D\right) \tag{8.9}$$

If one adds the temperature (T_{wet}) of a wet 'mimic' surface with no surface resistance to water loss, one can simplify this further (Guilioni et al. 2008; Leinonen et al. 2006). The precise formulation depends on whether the reference is wetted on one or both sides and whether the stomatal conductance is the same or different for the two leaf surfaces (Guilioni et al. 2008), however, for an amphistomatous (isolateral) leaf with a wet reference wetted on both sides this reduces to an estimate of the stomatal conductance (g_s) as

$$g_s = \left(\left(T_{dry} - T_s\right)/\left(T_s - T_{wet}\right)\right)\left[2\gamma g_{HR}/\left(\left(\gamma g_{HR}/g_{aW}\right) + 2s\right)\right] \tag{8.10}$$

where g_{aW} is the boundary layer conductance to water vapour for one side of the leaf. This equation is of the same form as Eq. 8.7, where the term in square brackets is a multiplier that depends primarily on the boundary layer conductance. Advantages of the use of reference surfaces include the fact that where all temperatures are measured by the same infrared thermometer/camera, errors in absolute temperature calibration can be eliminated.

In practice it is difficult to design a wet reference surface that remains wet continuously in hot, dry environments, though various designs have been proposed (Maes et al. 2016). Therefore most systems are based on the use of only dry references combined with humidity measurements (Eq. 8.9) with only a small reduction in accuracy (Leinonen et al. 2006).

2.4 Evaporation

Although it is the most difficult component of the surface energy balance to obtain from thermal sensing, rates of evapotranspiration (**ET**) can be conveniently estimated from remotely-sensed canopy temperature if appropriate assumptions are made (for a detailed discussion see Jones and Vaughan 2010). The best approach depends on the type of data available. The usual approach for satellite thermal imagery is to estimate regional **ET** as the residual term in the canopy energy balance using one-source energy balance algorithms such as SEBAL (Bastiaanssen et al. 1998a, b) and METRIC (Allen et al. 2007) or the more sophisticated two-source

algorithms that treat vegetated and non-vegetated areas separately (Kustas 1990; Kustas and Anderson 2009).

Other more approximate approaches can be valuable in many situations. One of these is to make use of the fact that the upper limit of **ET** is set by the available energy (R_n) and that for large well vegetated areas **ET** is often well approximated by the 'equilibrium evaporation rate' (McNaughton and Jarvis 1983) given by

$$\mathbf{ET} = 1.26\boldsymbol{s}\left(\mathbf{R}_n - \mathbf{G}\right)/\left(\lambda\left(\boldsymbol{s}+\gamma\right)\right) \tag{8.11}$$

in which λ is the latent heat of evaporation, **G** is heat storage in the soil and the constant 1.26 is known as the Priestley-Taylor constant. Where ground cover is not continuous it is necessary to modify the calculation by multiplying the result by a 'evaporative fraction' that takes account of the fraction of the surface that is evaporating at the potential rate (Sobrino et al. 2007). This can be achieved by making use of the linear relationship between **ET** and surface temperature and combining this with remotely sensed information on canopy cover.

Temperature gives a direct estimate of evaporation rate, while combination with information on the fractional canopy cover (f_{veg}, often estimated from the Normalised Difference Vegetation Index (NDVI) as obtained from multispectral sensing (Jones and Vaughan 2010)) allows one to further derive information on the degree of stomatal closure (Fig. 8.2).

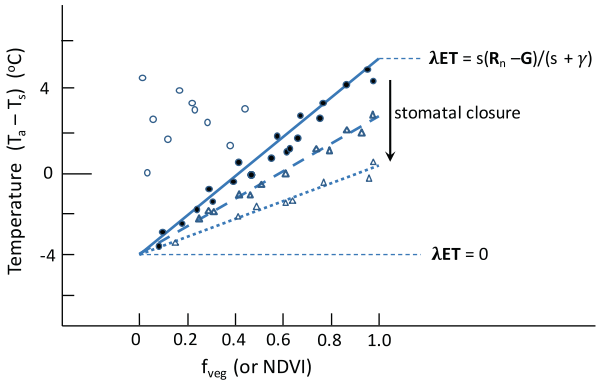

Fig. 8.2 Illustration of the general relationship between surface temperature and f_{veg} showing the trend to increasing Evaporation as canopy temperature decreases ($T_a - T_s$) increases. The solid circles show temperatures decrease as f_{veg} increases for dry soil and well watered plants, while the open triangles show the corresponding temperatures expected for water stressed vegetation showing increasing stomatal closure, increasing evaporation above that expected for transpiring vegetation alone. The open circles indicate samples with areas of wet soil or areas of open water. The line described by $\lambda\mathbf{ET} = s\ (\mathbf{R}_n - \mathbf{G})/(s + \gamma)$ indicates the temperatures that correspond to the potential rate of **ET** as determined by incoming energy

2.5 Dynamics

The dynamics of temperature changes can provide important ecophysiological information, whether at the scale of single leaves or plants, or at the plant community or even regional scales. At the single leaf scale it can be used as an alternative method for estimation of aerodynamic resistances.

The rate of change of temperature (dT/dt) depends on the tissue heat capacity ($\rho^* c_p^* \ell^*$) according to (Jones 2014)

$$dT/dt = \mathbf{S} / \left(\rho^* c_p^* \ell^* \right) \tag{8.12}$$

where the ρ^* and c_p^* are the density and heat capacity of the tissue material, and ℓ^* is the thickness. **S** is the rate of heat storage ignoring any **M** (=$\mathbf{R}_n$ − **C** − λ**E**). Following a step change in the environment that affects the rate of heat storage (such as a change in radiation), leaf temperature changes according to the following

$$T = T_2 - \left(T_2 - T_1 \right) \exp\left(-t / \tau \right) \tag{8.13}$$

where T_1 is the initial temperature and T_2 is the final equilibrium temperature and $\boldsymbol{\tau}$ is the time for c.63.2% of the total change to occur (known as the time constant). The time constant is given by

$$\tau = r^* c_p^* \ell^* / \left(r c_p \left(\left(1 / r_{HR} \right) + \left(s / \left(\gamma \left(r_{aW} + r_{\ell W} \right) \right) \right) \right) \right) \tag{8.14}$$

which for a non-transpiring surface where $r_{\ell W}$ is infinite, can be simplified and rearranged to give the aerodynamic resistance as

$$r_{aW} = \tau \rho c_p / \left(\left(\rho^* c_p^* \ell^* \right) - \tau \rho c_p / r_g \right) \tag{8.15}$$

Any suitable curve-fitting method can be used to estimate $\boldsymbol{\tau}$ (and hence r_{aW}) from the time course of temperature change after an environmental perturbation. For non-transpiring leaves (for example covered in petroleum jelly) this provides a potentially useful method for estimation of aerodynamic resistances, though it does not appear to have been used previously, probably because it requires accurate estimates of the heat capacity per unit area of tissue.

For more massive bodies such as fruits, and at larger scales for soils or regions, where temperature does not rapidly equilibrate throughout the body, the time course of surface temperature change is more complex. In this case the rate of change of surface temperature depends on the thermal conductance from the surface down into the depths and on the heat capacity of the material. A high thermal conductivity leads to surface temperature changing relatively slowly for a given energy input giving a material with a high thermal inertia (a strong resistance to temperature change).

The thermal dynamics of fruit surfaces can provide a useful tool for the detection of internal bruising or other damage. For example, Baranowski and colleagues (2008) have demonstrated that the thermal inertial was substantially greater for apple fruits with water core than for healthy fruits and that bruising can be readily detected (Baranowski et al. 2009). This difference results from the higher tissue water content and hence higher thermal conductivity in the damaged fruits.

The high conductivity of water lies behind the widespread application of the use of thermal inertia, as estimated from diurnal changes in surface temperature obtained from satellite imagery such as from MODIS which has two overpasses per day, as an indicator of soil moisture content (Verstraeten et al. 2006; Veroustraete et al. 2012; Zhang and Zhou 2016). Soils with higher water content have significantly greater thermal inertia together with a delay in the phase maximum.

Thermal inertia, otherwise known as thermal buffer capacity, has been proposed as an overall indicator of ecosystem integrity, summarising biotic and abiotic controls over energy flows in ecosystems (Aerts et al. 2004). In practice such a measure is, however, dominated by differences in vegetation, with forests and high soil moisture favouring high thermal inertia, while dry desert or grassland will have the lowest thermal inertia (most rapid temperature changes).

2.6 Boundary Layer Conductance

A number of approaches are available for estimation of the boundary layer conductance required for application of the methods described above. The value of g_H can be estimated at a leaf scale from aerodynamic theory using the relationships between wind speed and leaf size from

$$g_H = 6.62\left(u/l\right)^{0.5} \tag{8.16}$$

where u (m s^{-1}) is the wind speed and l (m) is the characteristic dimension of the leaf (Jones 2014). Alternatively, at a canopy scale, one can use wind profile theory (Monteith and Unsworth 2008; Jones 2014) to estimate g_{aH} as

$$g_H = \kappa^2 u_z / \left[\ln\left(\left(z-d\right)/z_o\right)\right]^2 \tag{8.17}$$

where κ is von Karmann's constant (=0.41), u_z is the wind speed at canopy height z, z_o is the roughness length (often assumed equal to 0.64*z), and d is the zero plane displacement (often assumed equal to 0.13*z).

A third approach that is well adapted to the leaf scale and for continuous monitoring in the field would be to calculate g_H from the temperatures of heated and unheated replica leaves mounted in the canopy (Brenner and Jarvis 1995).

A number of other, thermally-based approaches are at least theoretically possible. One of these is to use the cooling dynamics of heated leaves (as described above), while another would be to use thermal imagery with leaf 'mimic' reference surfaces wetted on 0, 1 or 2 surfaces.

2.7 Some Other Qualitative Applications

There has been a recent increase in the range of applications of thermal imaging in other eco-physiological studies. For example, thermal sensing can be a powerful tool for the study of plant disease, as many diseases lead to alterations in leaf temperature that can be detected by thermography, with the precise temperature responses and their sequence depending on the species/disease combination (Chaerle et al. 1999; Chaerle and Van Der Straeten 2001; Chaerle et al. 2004). Although mostly applied in a proximal or near-field situation for early detection of infections, there is evidence that useful information can be obtained from satellite or airborne thermal imagery (Lindenthal et al. 2005; Stoll et al. 2008).

Another area of interest has been in the study of thermogenic respiration in flowers (Skubatz et al. 1991; Bermadinger-Stebentheiner and Stabentheiner 1995; Lamprecht et al. 2002) as well as the role of solar heating in floral physiology, especially in arctic and alpine plants (Lamprecht et al. 2002, 2006; Dietrich and Korner 2014). Thermal imaging has also been used in forestry to investigate tree species diversity, with typical canopy temperatures being shown to vary between coniferous and broad-leaved forests (Leuzinger and Körner 2007).

3 Some Practical Aspects of Thermal Imaging

3.1 Absolute Accuracy

The absolute accuracy of thermal measurements is only critical for applications where absolute temperatures are required (e.g. for estimation of ET or stomatal conductance) and is not particularly critical for relative studies as in crop phenotyping. Most imagers currently available have thermal resolution fully adequate for plant water relations studies (i.e. <0.1 K), but their absolute accuracy is often no better than ±1 or 2 °C, so care is needed when absolute rather than relative values are of interest. This poor absolute accuracy is one of the strongest justifications for the use of reference surfaces in calculations because in such situations only temperature differences (which are generally available at higher precision) are required.

The accuracy of surface temperature measurement using thermography is critically dependent on the surface emissivity chosen and on settings for the

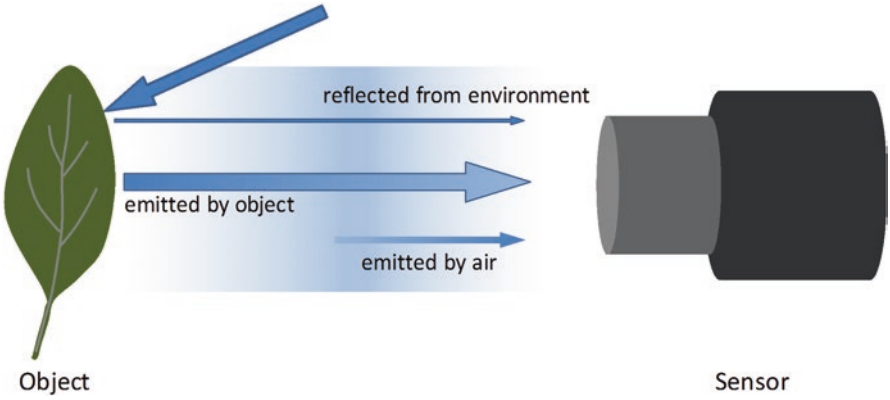

Fig. 8.3 Illustration of the radiation streams impinging on a thermal sensor, all of which need to be allowed for to obtain accurate temperature estimates. These corrections are commonly available in the thermal imaging software provided with the thermal cameras. The required corrections are greater, the more remote the sensor is from the object

'environmental temperature' and for the air temperature, humidity and distance between object and sensor. The temperature of a surface (T_s) is normally estimated by inversion of the following equation

$$R \cong \tau \, \varepsilon \, \sigma T_s^4 \tag{8.18}$$

where R is the total radiant flux density (W m^{-2}) received at unit area of sensor surface, τ is the longwave transmission by the atmosphere between the object and the sensor, ε is the surface emissivity and σ is the Stefan-Boltzmann constant (5.6697×10^{-8} W m^{-2} K^{-4}). Software in the sensor usually converts the received radiance to the radiance expected for the long wave band (correcting for the spectral sensitivity of the sensor) to produce an estimate of T_s. However, as shown in Fig. 8.3, the total longwave radiance arriving at the sensor is the sum of the thermal radiation emitted by the object (given by Eq. 8.18), the longwave radiation emitted by the atmosphere intervening between the object and the sensor, and the environmental longwave radiation reflected by the object towards the sensor, together with any of the emitted radiation absorbed by the intervening atmosphere.

For close-range sensing (less than about 5–10 m) the atmosphere is normally assumed to have a negligible effect on the at sensor radiance, though at high humidities it can be necessary to make some correction. The object emissivity also affects the temperature estimate, through its effect on both the emitted and reflected environmental radiation streams. The environmental radiation impinging on the object can have quite substantial effects on the apparent object temperature, especially for surfaces with emissivities substantially different from 1; for example, dry soils may have emissivities substantially below 0.9. The importance of emissivity to the correct estimation of temperature is illustrated by the fact that a 1% error in emissivity

can give rise to an error in the estimated temperature of more than 0.5 K (Jones and Vaughan 2010), suggesting that particular care is needed when comparing different types of surface in a single image.

3.2 Illumination of Object

The temperature of any surface is critically dependent on its exposure to the incoming solar radiation (Eq. 8.4). As pointed out by Jones et al. (2009) it follows therefore that leaves on the shaded side of trees will be cooler than those on the sunlit side. Similarly, even within a homogeneous canopy, the temperature of different leaves will vary over quite a wide range (Fuchs 1990) dependent on their incident radiation (which is a function of leaf orientation and any shading). A continuing discussion point is whether it is better to orient a thermal sensor with the sun behind the observer (to maximise the proportion of sunlit leaves), or whether better discrimination between plants is obtained when orienting the sensor towards the sun so that more of the observed leaves are shaded. The former has the advantages that temperatures are higher so that there is a greater temperature response for given differences in conductance, while conductances themselves tend also to be higher than for shaded leaves. The latter approach of studying shaded leaves has the advantage that temperature is much less sensitive to leaf orientation, but the lower temperatures and conductance can reduce sensitivity (Jones et al. 2002). Other studies, however, have suggested that thermal measurements on the top of canopies rather than the sides can produce more reliable estimates of conductance indices than viewing from the side (Grant et al. 2016), supporting the value of imagery from UAVs.

3.3 Design of Reference Surfaces

In order to give useful estimates of dry or wet reference temperatures for use in the equations outlined above, it is critical that the reference surface has similar radiative and aerodynamic properties to the surface of interest (e.g. a plant canopy). The choice of reference surfaces varies from the use of reference crops grown under similar conditions (Idso 1982) through simple temperature approximations (Irmak et al. 2000) to a range of physical references (Jones et al. 2017). For the dry reference it has frequently been proposed (Irmak et al. 2000; Ben-Gal et al. 2009; Meron et al. 2010) that approximating the dry reference as T_a + 5 °C is adequate in Mediterranean climates. Unfortunately as pointed out by Jones et al. (2017) there can in practice be substantial deviations from this simple approximation, especially in low radiation or high wind speed environments, leading to large errors in the derived estimates of conductance or **ET**. Similarly, large errors can arise if the spectral absorptance differs from the actual leaves (Jones et al. 2009) or where the size or thermal properties of the reference do not mimic the real leaves.

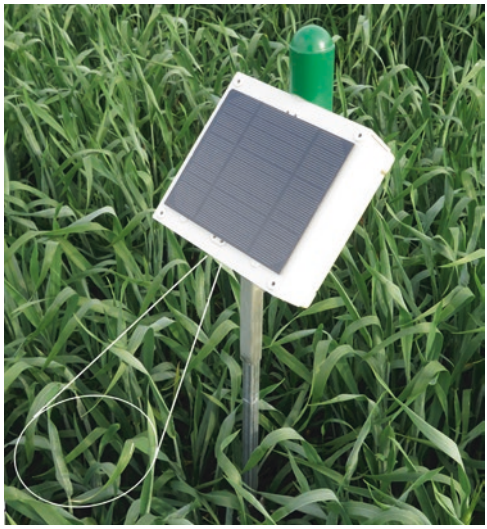

Fig. 8.4 Illustration of the ArduCrop dry reference sensor, showing the field of view of the downward-looking thermal infrared sensor and the dry reference hemisphere whose temperature is detected by an upward pointing infrared sensor. Power to drive the sensor and its connection to a local Wireless Sensor Network is provided by the solar panel shown. (see Jones et al. 2017, for further details)

Most reference surfaces have been constructed as flat leaf replicas made of green filter paper or similar material (Maes and Steppe 2012), but such surfaces cannot effectively replicate the range of illumination experienced by typical leaves in a plant canopy. In order to better represent the temperature of the range of leaves in a canopy, especially as solar elevation changes during the day, Jones et al. (2017) proposed use of the average temperature of a hemispherical surface (constructed of a half table-tennis ball; Fig. 8.4) on the basis that for a typical canopy with leaves oriented according to a spherical distribution (Monteith and Unsworth 2008) this would provide a closer approximation of the effective mean leaf temperature than would a flat surface.

Because the aerodynamic properties of the hemispherical reference may not exactly mimic those of leaves in a canopy, and also because of potential differences in solar absorptance from actual leaves, calculated estimates of conductance or **ET** may require modification by the use of a constant correction factor as outlined by Jones et al. (2017). A particular advantage of this type of reference is that it allows continuous monitoring of stomatal conductance and **ET**, allowing long-term and diurnal studies of water relations.

4 Conclusions

Thermal infrared sensing is becoming an increasingly powerful tool for the study of plant water relations and a range of other ecophysiological processes in both natural and agricultural ecosystems. Thermal imaging, whether from in-field sensors or from airborne sensors mounted on drones, aircraft or even satellites, has particular

advantages over the use of simple infrared thermometers with their single field of view because of the ability to make use of information about the variance of temperature of any object. A further advantage of imagery is that it can also be readily combined with multispectral or hyperspectral imagery to enhance the information about the object, for example through separating plant material from background and allowing the extraction of temperature of the plant material without confounding by background (Leinonen and Jones 2004). Nevertheless, arrays of simple cheap infrared thermometers, especially when combined with dry reference sensors (Jones et al. 2017), can be valuable for long term remote monitoring of evaporation and stomatal conductance. The recent advances in automated image analysis have the potential to greatly increase the power of thermal imagery for the study of plant water relations as it is becoming possible to avoid or reduce what is often a labour-intensive step in the application of thermography (Fuentes et al. 2012).

References

Aerts R, November E, Behailu M, Deckers J, Muys B (2004) Ecosystem thermal buffer capacity as an indicator of the restoration status of protected areas in the northern Ethiopian highlands. Restor Ecol 12:586–596

Allen RG, Tasumi M, Morse A, Trezza R (2007) Satellite-based energy balance for mapping evapotranspiration with internalized calibration (METRIC) – model. J Irrig Drain Eng 133:380–394

Baranowski P, Lipecki J, Mazurek W, Walczak RT (2008) Detection of watercore in 'Gloster' apples using thermography. Postharvest Biol Technol 47:358–366

Baranowski P, Mazurek W, Walczak W, Slawinski C (2009) Detection of early apple bruises using pulsed-phase thermography. Postharvest Biol Technol 53:91–100

Bastiaanssen WGM, Menentia M, Feddes RA, Holtslag AAM (1998a) A remote sensing surface energy balance algorithm for land (SEBAL). 1. Formulation. J Hydrol 213:198–212

Bastiaanssen WGM, Menentia M, Feddes RA, Holtslag AAM (1998b) A remote sensing surface energy balance algorithm for land (SEBAL) – 2. Validation. J Hydrol 213:213–229

Bendoricchio G, Jørgensen SE (1997) Exergy as goal function of ecosystems dynamic. Ecol Model 102:5–15

Ben-Gal A, Agam N, Alchanatis V, Cohen Y, Yermiyahu U, Zipori I, Presnov E, Sprintsin M, Dag A (2009) Evaluating water stress in irrigated olives: correlation of soil water status, tree water status, and thermal imagery. Irrig Sci 27:367–376

Bermadinger-Stebentheiner E, Stabentheiner A (1995) Dynamics of thermogenesis and structure of epidermal tiussues in inflorescences of *Arum maculatum*. New Phytol 131:41–50

Brenner AJ, Jarvis PG (1995) A heated leaf replica technique for determination of leaf boundary layer conductance in the field. Agric For Meteorol 72:261–275

Brough DW, Jones HG, Grace J (1986) Diurnal changes in water content of the stems of apple trees, as influenced by irrigation. Plant Cell Environ 9:1–7

Bryant RB, Moran MS (1999) Determining crop water stress from crop canopy temperature variability. ERIM International, Ann Arbor

Carter J, Brennan R, Wisniewski M (2001) Patterns of ice formation and movement in blackcurrant. HortSci 36:1027–1032

Chaerle L, Van Der Straeten D (2001) Seeing is believing: imaging techniques to monitor plant health. Biochim Biophys Acta-Gene Struct Express 1519:153–166

Chaerle L, Van Caeneghem W, Messens E, Lambers H, Van Montagu M, Van Der Straeten D (1999) Presymptomatic visulaization of plant-virus interactions by thermography. Nat Biotechnol 17:813–816

Chaerle L, Hagenbeek D, De Bruyne E, Valcke R, Van Der Straeten D (2004) Thermal and chlorophyll-fluorescence imaging distinguish plant-pathogen interactions at an early stage. Plant Cell Physiol 45:887–896

Dietrich L, Korner C (2014) Thermal imaging reveals massive heat accumulation in flowers across a broad spectrum of alpine taxa. Alpine Bot 124:27–35

Fuchs M (1990) Infrared measurement of canopy temperature and detection of plant water stress. Theor Appl Climatol 42:253–261

Fuchs M, Tanner CB (1966) Infrared thermometry of vegetation. Agron J 58:597–601

Fuentes S, De Bei R, Pech J, Tyerman S (2012) Computational water stress indices obtained from thermal image analysis of grapevine canopies. Irrig Sci 30:523–536

Fuller MP, Wisniewski M (1998) The use of infrared thermal imaging in the study of ice nucleation and freezing of plants. J Thermal Biol 23:81–89

Gardner BR, Blad BL, Watts DG (1981) Plant and air temperature in differentially irrigated corn. Agric Meteorol 25:201–207

Grant OM, Tronina L, Jones HG, Chaves MM (2007) Exploring thermal imaging variables for the detection of stress responses in grapevine under different irrigation regimes. J Exp Bot 58:815–825

Grant OM, Ochagavía H, Baluja J, Diago MP, Tardáguila J (2016) Thermal imaging to detect spatial and temporal variation in the water status of grapevine (*Vitis vinifera* L.). J Hort Sci Biotech 91:44–55

Guilioni L, Jones HG, Leinonen I, Lhomme JP (2008) On the relationships between stomatal resistance and leaf temperatures in thermography. Agric For Meteorol 148:1908–1912

Hamed F, Fuller MP, Telli G (2000) The pattern of freezing of grapevine shoots during early bud growth. Cryo-Lett 21:255–260

Idso SB (1982) Non-water-stressed baselines - a key to measuring and interpreting plant water-stress. Agric Meteorol 27:59–70

Irmak S, Dorota ZH, Bastug R (2000) Determination of crop water stress index for irrigation timing and yield estimation of corn. Agron J 92:1221–1227

Jackson RD, Reginato RJ, Idso SB (1977) Wheat canopy temperature: a practical tool for evaluating water requirements. Water Resour Res 13:651–656

Jackson RD, Idso SB, Reginato RJ, Pinter PJ Jr (1981) Canopy temperature as a crop water-stress indicator. Water Resour Res 17:1133–1138

Jones HG (1999a) Use of infrared thermometry for estimation of stomatal conductance as a possible aid to irrigation scheduling. Agric Forest Meteorol 95:139–149

Jones HG (1999b) Use of thermography for quantitative studies of spatial and temporal variation of stomatal conductance over leaf surfaces. Plant Cell Environ 22:1043–1055

Jones HG (2004) Application of thermal imaging and infrared sensing in plant physiology and ecophysiology. Adv Bot Res 41:107–163

Jones HG (2014) Plants and microclimate: a quantitative approach to environmental plant physiology, 3rd edn. Cambridge University Press, Cambridge

Jones HG, Vaughan RA (2010) Remote sensing of vegetation: principles, techniques, and applications. Oxford University Press, Oxford

Jones HG, Aikman D, McBurney TA (1997) Improvements to infra-red thermometry for irrigation scheduling. Acta Hort 449:259–266

Jones HG, Stoll M, Santos T, de Sousa C, Chaves MM, Grant OM (2002) Use of infrared thermography for monitoring stomatal closure in the field: application to grapevine. J Exp Bot 53:2249–2260

Jones HG, Serraj R, Loveys BR, Xiong LH, Wheaton A, Price AH (2009) Thermal infrared imaging of crop canopies for the remote diagnosis and quantification of plant responses to water stress in the field. Funct Plant Biol 36:978–989

Jones HG, Hutchinson PA, May T, Jamali H, Deery DM (2017) A practical method using a network of fixed infrared sensors for estimating crop canopy conductance and evaporation rate. Biosyst Eng 165:59–69

Keener ME, Kircher PL (1983) The use of canopy temperature as an indicator of drought stress in humid regions. Agric Meteorol 28:339–349
Kustas WP (1990) Estimates of evapotranspiration with one- and two-layer model of heat transfer over partial land cover. J Appl Meteorol 29:704–715
Kustas WP, Anderson M (2009) Advances in thermal infrared remote sensing for land surface modeling. Agric For Meteorol 149:2071–2081
Lamprecht I, Schmolz E, Blanco L, Romero CM (2002) Flower ovens: thermal investigations on heat producing plants. Thermochim Acta 391:107–118
Lamprecht I, Maierhofer C, Röllig M (2006) A thermographic promenade through the Berlin Botanic Garden. Thermochim Acta 446:4–10
Leigh A, Close JD, Ball MC, Siebke K, Nicotra AB (2006) Light cooling curves: measuring leaf temperature in sunlight. Funct Plant Biol 33:515–519
Leinonen I, Jones HG (2004) Combining thermal and visible imagery for estimating canopy temperature and identifying plant stress. J Exp Bot 55:1423–1431
Leinonen I, Grant OM, Tagliavia CP, Chaves MM, Jones HG (2006) Estimating stomatal conductance with thermal imagery. Plant Cell Environ 29:1508–1518
Leuzinger S, Körner C (2007) Tree species diversity affects canopy leaf temperatures in a mature temperate forest. Agric For Meteorol 146:29–37
Lindenthal M, Steiner U, Dehne H-W, Oerke E-C (2005) Effect of downy mildew development on transpiration of cucumber leaves visualised by digital infrared thermography. Phytopathology 95:233–240
Maes WH, Steppe K (2012) Estimating evapotranspiration and drought stress with ground-based thermal remote sensing in agriculture: a review. J Exp Bot 63:4671–4712
Maes WH, Baert A, Steppe K, Huete AR, Minchin PEH, Snelgar WP (2016) A new wet reference target method for continuous infraredthermography of vegetations. Agric For Meteorol 226:119–131
McNaughton KG, Jarvis PG (1983) Predicting the effects of vegetation changes on transpiration and evaporation. In: Kozlowski TT (ed) Water deficits and plant growth. Academic, New York, pp 1–47
Meron M, Alchanatis V, Cohen Y, Tsipris J, Orlov V (2010) Crop water stress mapping for site-specific irrigation by thermal imagery and artificial reference surfaces. Precis Agric 11:148–162
Monteith JL, Unsworth MH (2008) Principles of environmental physics, 3rd edn. Academic, Burlington
Qiu G-Y, Yano T, Momii K (1996) Estimation of plant transpiration by imitation leaf temperature – application of imitation leaf temperature for detection of crop water stress (II). Trans JSIDRE 185:43–49
Raschke K (1956) Über die physikalischen Beziehungen zwischen Wärmeübergangszahl, Strahlungsaustausch, Temperatur und transpiration eines Blattes [The physical relationships between heat-transfer coefficients, radiation exchange, temperature and transpiration of a leaf.]. Planta 48:200–238
Raschke K (1960) Heat transfer between the plant and the environment. Annu Rev Plant Physiol 11:111–126
Skubatz H, Nelson TA, Meeuse BJ, Bendich AJ (1991) Heat production in the Voodoo lily (*Sauromatum guttatum*) as monitored by infrared thermography. Plant Physiol 95:1084–1088
Sobrino JA, Gómez M, Jiménez-Muñoz JC, Olioso A (2007) Application of a simple algorithm to estimate daily evapotranspiration from NOAA–AVHRR images for the Iberian Peninsula. Remote Sens Environ 110:139–148
Stier JC, Filiault DL, Wisniewski M, Palta JP (2003) Visualization of freezing progression in turfgrasses using infrared video thermography. Crop Sci 43:415–420
Stoll M, Schultz HR, Baecker G, Berkelmann-Loehnertz B (2008) Early pathogen detection under different water status and the assessment of spray application in vineyards through the use of thermal imagery. Precis Agric 9:407–417
Tanner CB (1963) Plant temperatures. Agron J 55:210–211

Veroustraete F, Li Q, Verstraeten WW, Chen X, Bao A, Dong Q, Liu T, Willems P (2012) Soil moisture content retrieval based on apparent thermal inertia for Xinjiang province in China. Int J Remote Sens 33:3870–3885

Verstraeten WW, Veroustraete F, van der Sande CJ, Grootaers I, Feyen J (2006) Soil moisture retrieval using thermal inertia, determined with visible and thermal spaceborne data, validated for European forests. Remote Sens Environ 101:299–314

Zhang D, Zhou G (2016) Estimation of soil moisture from optical and thermal remote sensing: a review. Sensors 16:1308